

# Modeling the nonlinear photoluminescence intensity dependence observed in asymmetric GaN quantum discs with AlGaN barriers

K. H. Lee<sup>1</sup>, S. Birner<sup>2</sup>, J. H. Na<sup>1</sup>, R. A. Taylor<sup>1</sup>, J. W. Robinson<sup>1</sup>, J. H. Rice<sup>1</sup>, Y. S. Park<sup>3</sup>, C. M. Park<sup>3</sup>  
and T. W. Kang<sup>3</sup>

<sup>1</sup>Department of Physics, University of Oxford, Parks Road, Oxford, OX1 3PU, United Kingdom

<sup>2</sup>Walter Schottky Institute and Physics Department, Technical University of Munich, D-85748

Garching, Germany <sup>3</sup>Quantum-functional Semiconductor Research Center, Dongguk University, Seoul 100-715, South Korea

**Abstract** — By means of a 3D self-consistent numerical simulation we have calculated the wavefunctions and energies of the states in an asymmetric GaN quantum disc (Q-disc) system. Overall, good agreement between the modeling and experimental results were observed. Furthermore, modeling has provided an insight into the carrier dynamics of the Q-disc system. In particular, results from the modeling supports the view that the nonlinear relationship between PL intensity and excitation power was due to electron tunneling between the asymmetric GaN Q-discs.

**Index Terms** — Nanotechnology, simulation, quantum effect semiconductor devices, photoluminescence.

## I. INTRODUCTION

Nitride-based semiconductors have attracted much attention due to their potential application in optoelectronic devices such as lasers and light-emitting diodes [1]–[3]. In a parallel development, there has been a move towards low-dimensional optoelectronic devices, as these potentially lead to enhanced device performance, i.e. higher quantum efficiency and improved optical gain. Such low-dimensional semiconductor devices are grown using self-organized processes [4]–[5], which lead to high quality crystals and nanoscale geometries, but suffer from random distributions in size, composition, and position.

Self-organized nanocolumns are one promising solution because of the reproducibility of their geometry and alloy composition. They can be produced using conventional growth techniques without additional processing, which is a key issue for the realization of novel optoelectronic devices and applications. Since self-organized GaN nanocolumns were first fabricated on Al<sub>2</sub>O<sub>3</sub> by Yoshizawa et al. [6] GaN nanocolumns containing GaN quantum discs (Q-discs) embedded in AlGaN barriers have been fabricated by Ristić et. al. [7]–[8] in which strong carrier confinement effects have been observed.

Optical properties of asymmetric GaN Q-discs have been studied using both time-resolved and time-integrated

(TI) photoluminescence (PL) techniques [9]. This paper extends the previous experimental work by modeling the GaN Q-discs using nextnano<sup>3</sup> [10], a nanostructure simulator capable of solving the self-consistent 3D nonlinear Poisson-Schrödinger equation for wurtzite materials including strain, deformation potentials and piezo and pyroelectric charges. We employed a multi-band  $\mathbf{k}\cdot\mathbf{p}$  model to calculate the electron and hole wavefunctions in the Q-disc region. As a result we have gained an insight into the carrier confinement inside the Q-disc and the nonlinear relationship between PL intensity and excitation power. Schematic of the sample structure is shown in Fig. 1(a). The sample was grown on the top of GaN nanocolumns and consisted of ten periods of two alternating GaN Q-disc thicknesses separated by an Al<sub>0.5</sub>Ga<sub>0.5</sub>N barrier with a thickness of 1.2 nm. GaN Q-discs with 4 nm thickness were identified as ‘disc-A’ and with 2 nm thickness as ‘disc-B’.

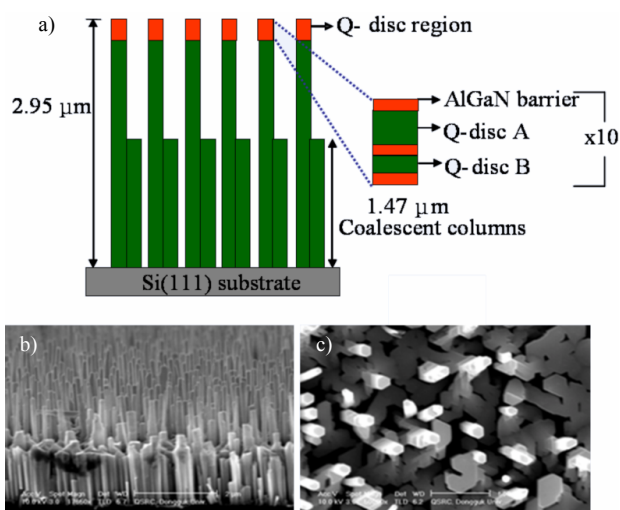


Fig. 1. (a) Schematic diagram of the Q-disc sample. (b) Cross-sectional and (c) plan view SEM images of the sample, showing the hexagonal columnar structure. The GaN Q-discs are embedded at the top region of the nanocolumn sample.

## II. Q-DISC EMBEDDED NANOCOLUMNS

### A. Growth

The nanocolumns were grown using plasma assisted molecular beam epitaxy on a Si(111) substrate without any buffer layer. The growth of GaN nanocolumns was performed under N-rich conditions [6],[11]. The Ga flux was controlled to a beam equivalent pressure of  $2 \times 10^{-7}$  Torr, which was approximately ten times smaller than that used for GaN epilayers ( $4 \times 10^{-6}$  Torr). The power and flow rate of the N plasma source were 350 W and 2.0 sccm, respectively. A growth temperature of 750 °C was used. The Al mole fraction of the AlGa<sub>0.5</sub>N barrier was deduced by means of a linear interpolation of Al content determined by high resolution x-ray diffraction as a function of Al cell temperature in the limit of nanocolumns. Cross-sectional and plan view SEM images of the nanocolumns are depicted in Figs. 1(b) and 1(c). The hexagonal GaN nanocolumns exhibited various diameters ranging from 50 to 120 nm and a density of  $1 \times 10^9 \text{ cm}^{-2}$ .

### B. Experimental Setup

The Q-discs were excited using a frequency-tripled Ti:sapphire laser at 275 nm, with a 150 fs pulsewidth and a repetition frequency of 76 MHz. The sample was mounted in a continuous-flow helium cryostat allowing the temperature to be varied from room temperature to 4 K. A  $36 \times$  reflecting objective was held above the cryostat to both focus the incident laser beam to a spot size of  $\sim 2 \mu\text{m}$  and to collect the resulting luminescence. The PL was dispersed by a 0.3 m spectrograph, which was equipped with a 1200 grooves/mm grating giving a spectral resolution of  $\sim 0.7 \text{ meV}$ . The PL was detected by a Peltier-cooled CCD.

## III. EXPERIMENTAL RESULTS

For a detailed discussion of the experimental results the reader is referred to Ref. [9]. In this section, we discuss the results that are of relevance to the modeling.

The TI-PL spectrum of GaN nanocolumns with and without Q-discs was measured and this is shown in Fig. 2(a). The spectrum showed an emission peak at 3.58 eV for GaN nanocolumns without Q-discs (labeled C), while for nanocolumns containing Q-discs peak emissions were observed at 3.465 and 3.544 eV. These were identified to originate from disc-A and disc-B, respectively (labeled DA and DB). Figure 2(b) shows the excitation-power dependence of the GaN Q-discs. The

spectra shows that with increase in excitation DA grows more rapidly than DB.

This observation is further illustrated in the plot of PL intensity versus laser excitation power, as shown in Fig. 2(c). The PL intensity of DB is proportional to the excitation power. This is in contrast to DA, whose intensity shows a superlinear (quadratic) dependence for excitation powers  $> 3.1 \text{ mW}$ . In Ref. [9] this effect has been suggested as a result of electrons and holes created in disc-B tunneling into disc-A. It was proposed that most of the electrons in disc-B tunnel into disc-A before they can recombine with holes in disc-B [12]-[13]. This results in an overpopulation of the excited electron bound states in disc-A. Such tunneling transitions potentially give rise to an increase in the radiative recombination in disc-A, resulting in the nonlinear relationship between PL intensity and excitation power.

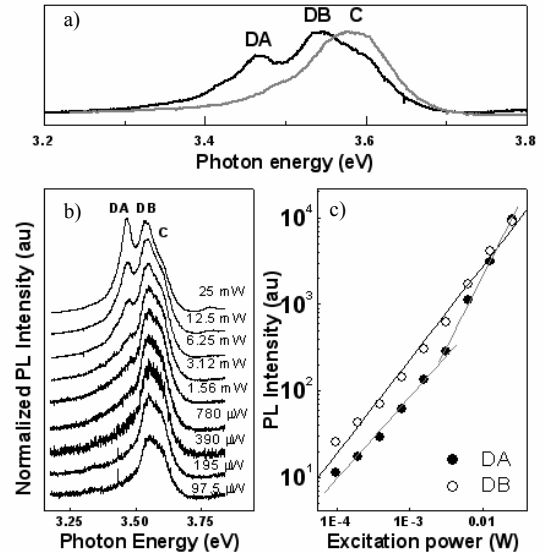


Fig. 2. (a) TI-PL of GaN nanocolumns without (grey line-trace) and with Q-discs (black line-trace) recorded at 4 K (6.25 mW). (b) TI-PL from GaN nanocolumns containing Q-discs, recorded as a function of excitation power. (c) Plot of photoluminescence intensity vs. excitation power.

## IV. MODELING

The electron and hole wavefunctions of our Q-discs were calculated on a 50 nm diameter nanocolumn. The  $\text{Al}_{0.5}\text{Ga}_{0.5}\text{N}$  barriers were modeled as 1 nm thick cylindrical discs. These were inserted in between the cylindrical shaped GaN discs that were alternating in thickness (2 nm, 4 nm) to correctly reproduce the A- and B-discs of our grown samples. The Al alloy profile of the AlGa<sub>0.5</sub>N discs was assumed to be uniform. The geometry of the model is shown in Fig. 3.

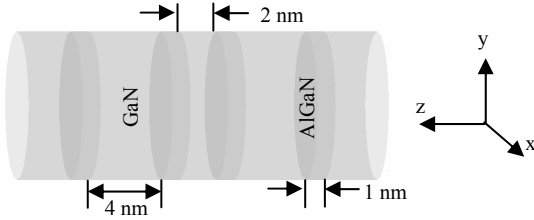


Fig. 3. Schematic of the model with the dimensions included.

The three-dimensional **nextnano**<sup>3</sup> calculations involved the following steps:

- 1) Calculate the strain.
- 2) Calculate the piezoelectric charges from the strain and pyroelectric charges.
- 3) Solve the Poisson equation including piezoelectric and pyroelectric charges to obtain the electrostatic potential.
- 4) Solve from the resulting electrostatic potential the Schrödinger equation.

These calculations were done in a self-consistent manner. The fully strained Q-discs were simulated by minimization of the elastic energy within a continuum model approach that takes into account the symmetry of the hexagonal crystal structure.

In order to calculate the wavefunctions we considered a one-band model for the electrons and a six-band **k.p** Hamiltonian for the holes. This can be justified as both GaN and AlN have large band gaps and therefore the coupling between the conduction and valence bands can be neglected [14]. The shift and splitting of the band edges due to strain were automatically included in these Hamiltonians by using the relevant deformation potentials. In addition, we assumed that the wavefunction was negligible beyond the nanocolumn region. Numerically this was achieved by using Dirichlet boundary conditions for the Schrödinger equation at the nanocolumn boundaries. This assumption was based on the previous observations of strong carrier confinement within the nanocolumns [7]-[8].

It is not possible yet to treat the strain at the air-semiconductor interface correctly. The implementation of a suitable model into **nextnano**<sup>3</sup> is currently under development. So far, we assumed that the atoms at the GaN boundary of the nanocolumn were not allowed to relax into the surrounding air material.

## V. RESULTS AND DISCUSSION

The calculated strain tensor and piezoelectric field for the Q-discs were calculated. For disc-B the piezoelectric field was calculated to  $\sim 4$  MV cm<sup>-1</sup>. This large piezoelectric field is consistent with the expected behavior

of wurtzite III-V nitrides, which are known to possess the largest piezoelectric constants amongst tetrahedrally bonded materials [15]. The effect of strain and piezoelectric fields on the Q-disc is evident in the tilting of the conduction and valence bands. Visualization of the bands along the z-direction is shown in Fig. 4 and is consistent with the results from other modeling studies of AlGaIn/GaN heterojunctions [14],[16]. Hence, the simulated model agrees with other theoretical predictions.

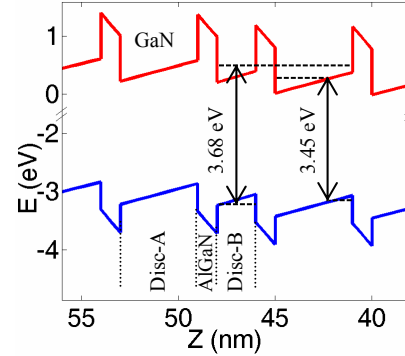


Fig. 4. Conduction and valence band along the z-axis, showing the tilt in the bands due to strain and piezoelectric field. The electron and hole energy levels are marked on the figure.

Following the calculation of the conduction and valence bands the wavefunctions were determined. The probability densities of the lowest energy states in the conduction and the valence band for disc-A and disc-B are presented in Fig. 5. The energy separation between the hole and the electron was calculated to be 3.45 eV for disc-A and 3.68 eV for disc-B. This is in good agreement with the observed peak values, given the simplification in the geometry and the uncertainty of the parameters.

Several important features can be observed from Fig. 5. Firstly, the peaks of the wavefunctions are shifted, relative to the centre of the disc region, with the direction of the shift being different for the electrons and holes. This is due to the tilting of the bands [16]. This has important consequences as it ‘localizes’ the electrons and holes to different spatial regions (towards the opposite ends of the Q-disc along the z-direction). This reduces the overlap integral between the electron and hole wavefunction, which is an important parameter as it determines optical properties such as the exciton lifetime.

Secondly, the modeling shows that only the electron in disc-B is able to tunnel through the AlGaIn barrier to form a state in disc-A. This is because the energy of the electron lies above the triangular region of potential as indicated in Fig. 4, and it ‘sees’ a 1 nm thick barrier. The converse is not true as the electron energy in disc-A is lower (by  $\sim 0.15$  eV) and the energy of the electron lies

within the triangular region of potential. It ‘sees’ a significantly thick barrier and the electron cannot tunnel through to the disc-B. This result adds support to our previous work [9], in which we have suggested that tunneling transitions were responsible for the increase in the radiative recombination in disc-A, resulting in the nonlinear relationship between PL intensity and excitation power. Furthermore we have modeled a 80 nm diameter Q-disc and found that the tunneling was still present, but at lower probability, as expected.

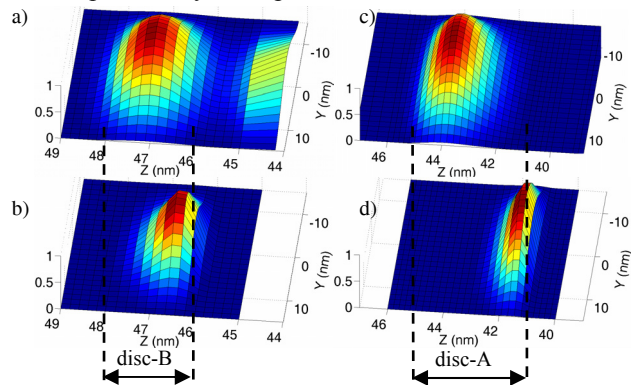


Fig. 5. Visualization of the (a) electron and (b) hole probability densities in disc-B and of the (c) electron and (d) hole probability densities in disc-A. Disc-B is between  $48 > z > 46$  nm and disc-A is between  $45 > z > 41$  nm. Red regions correspond to high probability. The tunneling of the electron in disc-B is evident in (a). The 2D slices of the 3D wavefunctions were taken along the center line in x-direction ( $x = 0$  nm).

## VII. CONCLUSION

We have calculated the wavefunctions and energies of the lowest states in coupled GaN Q-discs by means of a sophisticated 3D numerical simulation. Good agreement was achieved between the experimental and modeled results. In addition, modeling has provided new insights into the carrier dynamics of these Q-discs, demonstrating that the tunneling between the two types of Q-discs plays an important role in the optical properties of these nanocolumns.

## ACKNOWLEDGEMENT

This work was supported by the Foresight LINK Award *Nanoelectronics at the Quantum Edge* EPSRC GR/R66029/01 and by Hitachi Cambridge Laboratory. Authors at the Quantum Functional Semiconductor Research Center at Dongguk University acknowledge the support of the Korea Science and Engineering Foundation. K.H. Lee acknowledges the support of the University College old members fund scholarship and the Clarendon Fund bursary.

## REFERENCES

- [1] S. Nakamura, et al., “High-brightness InGaN blue, green, and yellow light-emitting diodes with quantum well structures” *Jpn. J. Appl. Phys.*, vol. 34, pp. L797-L799, 1995.
- [2] S. Nakamura, et al., “Superbright green InGaN single-quantum-well-structure light-emitting diodes” *Jpn. J. Appl. Phys.*, part 2, vol. 34, pp. L1332-L1335, 1995.
- [3] A. Ponce and D. P. Bour, “Nitride-based semiconductors for blue and green light-emitting devices” *Nature*, vol. 368, pp. 351-359, 1997.
- [4] D. J. Eaglesham and M. Cerullo, “Dislocation-Free Stranski-Krastanov Growth of Ge on Si” *Phys. Rev. Lett.*, vol. 64, pp.1943-1946, 1990.
- [5] J. C. Wang, et al. “High-quality GaN nanowires synthesized using a CVD approach” *Appl. Phys. A: Mater. Sci. Process.*, vol. 75, 2002.
- [6] M. Yoshizawa, et al. “Self-organization of GaN/Al<sub>0.18</sub>Ga<sub>0.82</sub>N Multi-layer Nano-columns on (0001) Al<sub>2</sub>O<sub>3</sub> by RF Molecular Beam Epitaxy for Fabricating GaN Quantum Disks” *J. Cryst. Growth*, vol. 189/190, pp.138-141, 1998.
- [7] M. A. Ristić, et al., “AlGaIn Nanocolumns Grown by Molecular Beam Epitaxy: Optical and Structural Characterization” *Phys. Status Solidi A*, vol.192, pp. 60-66, 2002.
- [8] M. A. Ristić, et al., “Characterization of GaN quantum discs embedded in Al<sub>x</sub>Ga<sub>1-x</sub>N nanocolumns grown by molecular beam epitaxy” *Phys. Rev. B*, vol. 68, 125305, 2003.
- [9] J. H. Na, et al., “Time-resolved and time-integrated photoluminescence studies of coupled asymmetric GaN quantum discs embedded in AlGaIn barriers” *Appl. Phys. Lett.*, vol. 86, 083109, 2005.
- [10] nextnano<sup>3</sup> device simulator: The program is available at [www.wsi.tum.de/nextnano3](http://www.wsi.tum.de/nextnano3) and [www.nextnano.de](http://www.nextnano.de).
- [11] J. Sanchez-Paramo, et al., “Structural and optical characterization of intrinsic GaN nanocolumns” *Physica E*, vol. 13, pp. 1070-1073, 2002.
- [12] R. Ferreira and G. Bastard, “Evaluation of some scattering times for electrons in unbiased and biased single- and multiple-quantum-well structures”, *Phys. Rev. B*, vol. 40, pp. 1074-1086, 1989.
- [13] M. F. Krol, et al., S. Ten, M. J. Hayduk, G. Khitrova, and N. Peyghambarian, “Sub-picosecond hole tunneling by nonresonant delocalization in asymmetric double quantum wells” *Phys. Rev. B*, vol. 52, 14344, 1995.
- [14] V. A. Fonoberov and A. A. Balandin, “Excitonic properties of strained wurtzite and zinc-blende GaN/Al<sub>x</sub>Ga<sub>1-x</sub>N quantum dots”, *J. Appl. Phys.*, vol. 94, no. 11, pp. 7178-7186, 2003.
- [15] F. Bernardini, et al., “Spontaneous Polarization and piezoelectric constants of III-V nitrides”, *Phys. Rev. B*, vol. 56, pp. R10024-R10037, 1994.
- [16] C. A. Flory and G. Hasnain, “Modeling of GaN Optoelectronic Devices and Strain-Induced Piezoelectric Effects” *IEEE J. Quantum Electron.*, vol. 37, no. 2, pp. 244-253, 2001.